Nearly localized nature of f electrons in CeTIn$_5$ (T=Rh, Ir)

Shin-ichi Fujimori, Tetsuo Okane, Jun Okamoto, Kazutoshi Mamiya, and Yasuji Muramatsu
Synchrotron Radiation Research Center, Japan Atomic Energy Research Institute, SPring-8, Mikazuki, Hyogo 679-5148, Japan

Atsushi Fujimori
Department of Complexity Science and Engineering, University of Tokyo, Bunkyo-ku, Tokyo 113-0033, Japan and Synchrotron Radiation Research Center, Japan Atomic Energy Research Institute, SPring-8, Mikazuki, Hyogo 679-5148, Japan

Hisatomo Harima
ISIR-SANKEN, Osaka University, Ibaraki, Osaka 567-0043, Japan

Dai Aoki, Shugo Ikeda, Hiroaki Shishido, and Yoshifumi Tokiwa
Graduate School of Science, Osaka University, Toyonaka, Osaka 560-0043, Japan

Yoshinori Haga
Advanced Science Research Center, Japan Atomic Energy Research Institute, Tokai, Ibaraki 319-1195, Japan

Yoshichika Ōnuki
Graduate School of Science, Osaka University, Toyonaka, Osaka 560-0043, Japan and Advanced Science Research Center, Japan Atomic Energy Research Institute, Tokai, Ibaraki 319-1195, Japan

(Received 15 June 2002; revised manuscript received 6 February 2003; published 14 April 2003)

We have performed angle-resolved photoemission spectroscopy ($h\nu$=21.2,40.8 eV), Ce $3d$-$4f$ resonant photoemission spectroscopy ($h\nu\sim$881 eV), and Ce $3d$ x-ray absorption spectroscopy studies on the layered cerium compounds CeTIn$_5$ (T=Rh and Ir), which show competition between superconductivity and antiferromagnetism. The results suggest that the Ce $4f$ electrons in both compounds are nearly localized. We have found that although the Ce $4f$ electrons in the superconducting CeIrIn$_5$ are more delocalized than those in the antiferromagnetic CeRhIn$_5$, their electronic structures are very similar to each other.

DOI: 10.1103/PhysRevB.67.144507 PACS number(s): 79.60.−i, 71.27.+a, 71.18.+y

I. INTRODUCTION

The relationship between magnetism and superconductivity has attracted much attention. Especially, some magnetic f-electron compounds show superconductivity under high pressure, suggesting that magnetic interactions may play essential roles in the superconductivity.[1,2] CeTIn$_5$ (T=Rh and Ir) are a recently synthesized class of Ce-based compounds. CeIrIn$_5$ shows superconductivity at ambient pressure while CeRhIn$_5$ is antiferromagnetic at ambient pressure and shows superconductivity under high pressure. They are thought to be located near the quantum critical point (QCP) in Doniach's phase diagram, and are good target materials to study how the magnetic interactions are involved in the pairing mechanism.

The CeTIn$_5$ compounds crystallize in the tetragonal HoCoGa$_5$-type structure, which can be viewed as an alternating stack of the CeIn$_3$ and TIn$_2$ layers. Therefore, they can be regarded as a quasi-two-dimensional version of CeIn$_3$, which is a typical pressure-induced superconductor at P_C $\sim$25 kbar and T_C=0.2 K.[3] CeRhIn$_5$ is a heavy fermion (HF) antiferromagnet with T_N=3.8 K at ambient pressure.[4] According to their lattice constants, the CeIn$_3$ layers experience a chemical pressure of $\sim$14 kbar relative to bulk CeIn$_3$. Hegger *et al.*[4] have discovered that CeRhIn$_5$ undergoes a superconducting transition at $P_C\sim$16.3 kbar and T_C=2 K. This P_C is actually lower than that of CeIn$_3$, supporting that CeRhIn$_5$ corresponds to CeIn$_3$ under high pressure. Alver *et al.*[5] have measured de Haas-van Alphen (dHvA) effect in Ce$_x$La$_{1-x}$RhIn$_5$, and found that the sizes and topologies of their Fermi surface are nearly independent of x. In addition, Shishido *et al.*[6] have performed a detailed dHvA study on CeRhIn$_5$ and LaRhIn$_5$, and showed that three-dimensional topologies of their Fermi surface are also essentially the same. These results suggest that the Ce $4f$ electrons are localized in CeRhIn$_5$. Meanwhile, CeIrIn$_5$ has a small lattice constant along the c axis compared with that of CeRhIn$_5$, and corresponds to CeRhIn$_5$ under pressure. CeIrIn$_5$ is a HF superconductor with T_C=0.4 K at ambient pressure, which is again consistent with the picture that the CeIn$_3$ layers in CeIrIn$_5$ experience a high chemical pressure compared with those in CeRhIn$_5$.[7] Haga *et al.*[8] have measured dHvA oscillation in this compound, and found that the topology and size of the Fermi surface are well explained by the itinerant $4f$ electron model. In addition, Zheng *et al.*[9] have made a nuclear quadrupole resonance (NQR) study of CeIrIn$_5$, and concluded that $4f$ electrons in this compound are much more itinerant than in the other known Ce-based HF compounds. Moore *et al.*[10] have performed an angle-resolved photoelectron spectroscopy (ARPES) study for CeRhIn$_5$, and suggested that the results can be understood by itinerant $4f$-electron model in contrast to the results of dHvA experiments. In this paper, we report on the results of comparative photoemission and x-ray absorption experiments on those

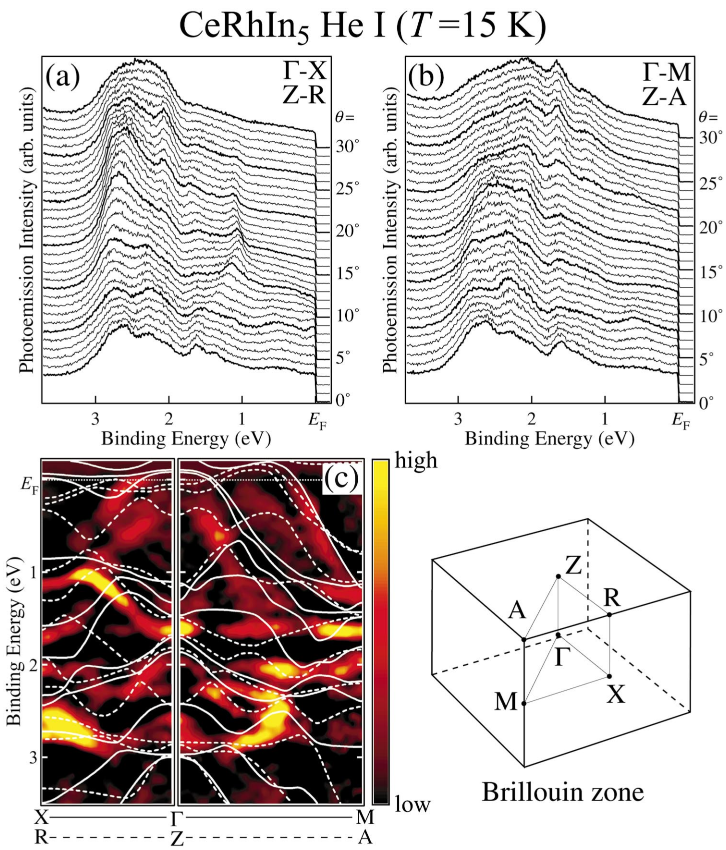

FIG. 1. (Color) ARPES spectra of $CeRhIn_5$ measured with He Iα radiation. (a) EDC's along the Γ-X(Z-R) direction. (b) EDC's along the Γ-M(Z-A) direction. (c) Comparison between the experimental image of band structure and the result of the band structure calculation. The Brillouin zone of Ce$T$$In_5$ is also shown.

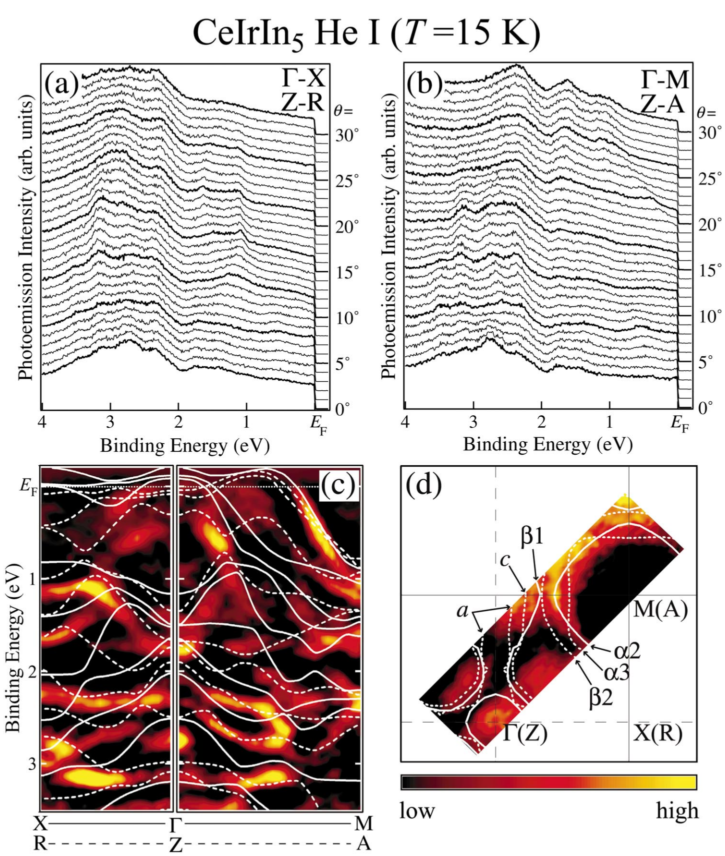

FIG. 2. (Color) ARPES spectra of $CeIrIn_5$ measured with He Iα radiation. (a) EDC's along the Γ-X(Z-R) direction. (b) EDC's along the Γ-M(Z-A) direction. (c) Comparison between the experimental image of band structure and the result of the band structure calculation. (d) Two-dimensional intensity map of the intensity at E_F with the calculated Fermi surfaces.

compounds, to understand their electronic structures. ARPES experiment using a monochromatized He discharge light ($h\nu$=21.2,40.8 eV) and resonant photoelectron spectroscopy (RPES) experiment using soft x-ray synchrotron radiation ($h\nu$=870,881.2 eV) were performed. The present results suggest that Ce $4f$ electrons in both compounds are relatively localized in the measured temperature range (~15 K). In addition, we have found that Ce $4f$ electronic states in $CeIrIn_5$ and $CeIrIn_5$ are very similar to each other.

II. EXPERIMENT

Single crystals of $CeRhIn_5$ and $CeIrIn_5$ were grown by the self-flux method described in Ref. 4. Clean sample surfaces were obtained by *in situ* cleaving the samples parallel to the *a*-*b* plane. The ARPES experiments were performed using a spectrometer equipped with a GAMMADATA-SCIENTA SES2002 electron analyzer and a monochromatized GAMMADATA-SCIENTA VUV-5000 He lamp. The overall energy resolution of the ARPES measurements was set to about 15 meV. The RPES experiments utilized soft x-rays from beamline BL23SU of SPring-8, and the overall energy resolution was about 200 meV. X-ray absorption spectroscopy (XAS) spectra were also recorded using total electron yield method. The sample temperature was kept at 15 K during the course of the measurements. The position of the Fermi level (E_F) is carefully determined referring to the evaporated gold film. Full-potential-linear-augmented-plane-wave (FLAPW) band structure calculations were performed to compare them with the ARPES spectra. The calculations were done for the paramagnetic phase. The details of the calculations are described in Ref. 8.

III. RESULTS AND DISCUSSION

First, we present the ARPES spectra of $CeRhIn_5$, measured with He Iα radiation to show the overall energy band structure of this compound. Figure 1 shows the energy distribution curves (EDC's) measured along the Γ-X(Z-R) (a) and Γ-M(Z-A) (b) high symmetry directions. Some dispersive features are clearly observed. To see these feature more clearly and to compare them with the results of the FLAPW band structure calculations, we have derived the ''image'' of the band structure by taking the second derivatives of the spectra. We have combined the second derivative of the EDC's and momentum distribution curves (MDC's) for making the image of the band structures as follows. The EDC's for $E_B<0.01$ eV, where the Fermi edge cutoff starts, were linearly extrapolated to above E_F before taking the second derivative to avoid the strong contributions from the Fermi cutoff. The second derivatives of the MDC's are not influenced by the Fermi edge cutoff. Then, the second derivatives of the EDC's and MDC's were added with a certain ratio so that the resulting plot clearly resolves as many bands as possible. Figure 1(c) shows comparison between the image of the band structure derived using this method and the calculated energy band structure, which treats the Ce $4f$ electrons are as being itinerant. The red and yellow part in the image corresponds to the experimental peak position, and the solid and dashed lines are the calculated energy band dispersions to be compared with the experiment. In the Γ-X(Z-R) direction, the prominent dispersive features at 1–1.7 eV show correspondence to the calculated energy band dispersions, although their energy positions are slightly different. The calculation suggests that these features are originated mainly from In *p* states. The complicated energy band dispersions, originated from Rh *d*-derived states in the range of 2–3 eV, also show very good correspondence to the calculation. In the Γ-M(Z-A) direction, one structure is crossing the Fermi level around the *M* point in the experiment. This structure also well corresponds to the calculation. However, nearly flat bands located near E_F for the Γ-X direction, which are derived mainly from the Ce $4f$ states, were not clearly observed in these spectra.

Figure 2 shows the EDC's of $CeIrIn_5$ measured along the Γ-X(Z-R) (a) and Γ-M(Z-A) (b) high symmetry direction. The overall angular dependence of the EDC's is very similar to those of $CeRhIn_5$, except for the Ir *d*-derived states at 2–3.5 eV. Figure 2(c) shows comparison between the experimental and theoretical band dispersions. Here, as in the case of $CeRhIn_5$, most of the experimentally observed energy dispersions correspond well to the calculated energy dispersions, but the Ce $4f$ derived flat bands are again not clearly observed. To obtain the information about the Fermi surface (FS) of this compound, we have made two-dimensional (2D) mapping of the photoemission intensity at E_F. Figure 2 (d) shows the photoemission intensity at E_F in the momentum space. The calculated FS's are also shown by the solid (Γ-X-M plane) and dotted (Z-R-A plane) lines. The contribution from 2D cylindrical FS centered at M(A) is observed in the image. In the band structure calculation, there exists three 2D cylindrical FS's in these planes, and α_2 and α_3 seem to correspond to the observed FS. The calculation indicates that the contributions from Ce $4f$ states are very small in these two FS's. We have observed similar 2D cylindrical FS in the ARPES spectra of $CeRhIn_5$ also. Hall *et al.*[11] performed a dHvA experiment on $CeRhIn_5$, and pointed out the overall similarity of the topology of the quasi-2D FS between $CeRhIn_5$ and $CeIrIn_5$. On the other hand, Shishido *et al.*[6] have also performed dHvA study on $CeRhIn_5$, and indicated that although the topologies of FS's are similar between $CeRhIn_5$ and $CeIrIn_5$, the sizes of FS's are smaller in $CeRhIn_5$ than in $CeIrIn_5$. For example, the size of α_2 branch is reduced to be about 84% on going from $CeIrIn_5$ to $CeRhIn_5$. They suggest that this difference in the size of FS's reflects the difference between the ''localized'' and ''delocalized'' $4f$ FS in the ground state. Although it is not easy to exactly determine the size of these FS's from ARPES, we have made the estimation of the their size from ARPES. The k_F of α_2 branch for Γ-M direction estimated from ARPES are about 0.41 ± 0.01 Å^{-1} and 0.44 ± 0.01 Å^{-1} for $CeRhIn_5$ and $CeIrIn_5$ respectively. Therefore, k_F of $CeRhIn_5$ is about 93% of that of $CeIrIn_5$. If the shape of these FS's are unchanged, the size of these branches in $CeRhIn_5$ are estimated to be about 88% of those of $CeIrIn_5$. Therefore, if we limit our argument on the shape and size of the α_2 branch, it seems that the results of dHvA on $CeRhIn_5$ and $CeIrIn_5$ are

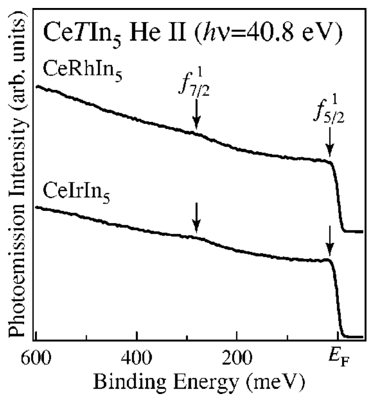

FIG. 3. AIPES spectra of $CeRhIn_5$ (a) and $CeIrIn_5$ (b) measured with He IIα radiation.

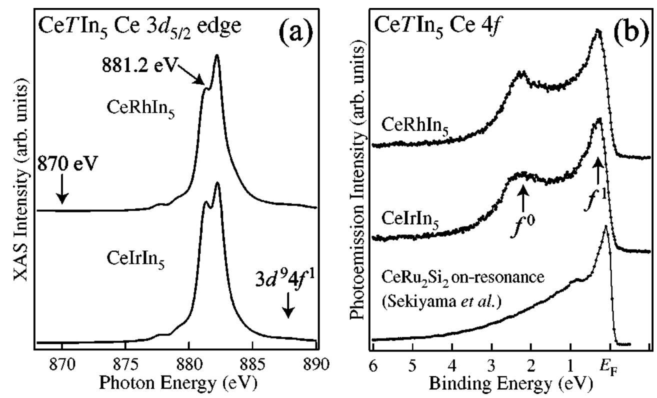

FIG. 4. (a)Ce $3d_{5/2}$ x-ray absorption spectra and (b) Ce 4f partial spectra of $CeRhIn_5$ and $CeIrIn_5$ taken at $T=15$ K.

consistent with our ARPES results. On the other hand, the FS's designated as β_1 and β_2, which were also detected in the dHvA experiment, are not clearly observed in the ARPES study. In addition, the "networklike" FS's designated as a, which has large contributions from the Ce 4f states, were not also clearly observed. Therefore, the calculation well reproduces the FS's with smaller 4f contributions, but fails to describe those with higher 4f contributions. In the dHvA experiment, the small spherical FS with cyclotron mass $m_c^* = 6.3m_0$ (designated as γ in Ref. 8) was observed, and its origin was not clear.[8] Here, we observed small FS centered at Γ, and this might be related to branch γ.

To identify the Ce 4f derived component, we have measured the ARPES spectra using He IIα radiation. The atomic calculation suggests that the cross section of Ce 4f electrons for the He IIα radiation is about six times larger than that for He Iα radiation, while those of transition metal d and In s,p states are almost the same between He Iα and He IIα.[14] Figure 3 shows the angle integrated photoemission (AIPES) spectra of (a) $CeRhIn_5$ and (b) $CeIrIn_5$, obtained by adding the ARPES spectra. A very weak structure is observed at the Fermi level, and is considered to be originated from the Ce $4f^1_{5/2}$ final state or the tail of the Kondo peak. Another weak structure, located at about 280 meV, is originated from the $4f^1_{7/2}$ final state side band. The weakness of the contributions from the 4f states at the Fermi level suggests that the hybridization between the Ce 4f and In 4p states is very weak in these compounds. A closer examination reveals that the intensity at the Fermi level is slightly larger in $CeIrIn_5$ than that in $CeRhIn_5$, suggesting that the hybridization is a little stronger in $CeIrIn_5$ than in $CeRhIn_5$.

To further study contributions from the Ce 4f states, we have performed 3d-4f resonant photoemission experiments on these compounds. This method utilizes the large enhancement of the Ce 4f cross section near the Ce 3d core-absorption threshold. Figure 4(a) shows Ce $3d_{5/2}$ XAS spectra of $CeTIn_5$. We have constructed the Ce 4f derived spectra by subtracting the weak off-resonance spectra ($h\nu = 870$ eV) from the on-resonance spectra ($h\nu = 881.2$ eV). Figure 4(b) shows the Ce 4f derived spectra of $CeTIn_5$. The spectra consist of the f^1 final-state peak located just below the Fermi level and the f^0 final-state peak at about 2 eV. These spectral features have been observed in other Ce-based compounds, and understood within the framework of the single impurity Anderson model (SIAM).[12] According to SIAM, the stronger the f electrons hybridize with conduction electrons, the stronger the f^1 peak becomes. Here, the intensity of the f^0 final state peak, located at 2 eV, is very strong compared with other HF Ce compounds measured so far. For example, we have shown the on-resonance spectra of $CeRu_2Si_2$ with a low Kondo temperature ($T_K = 22$ K), namely, with weakly hybridized 4f electrons, measured by Sekiyama *et al.*,[13] where the f^0 final state peak intensity is extremely weak. In addition, the peak intensity of the $3d^94f^1$ final state in the XAS spectrum of $CeIrIn_5$ [Fig. 4(a)], which is originated from the $4f^0$ state in the ground state, is almost invisible, suggesting that the number of Ce 4f electrons in the initial state is very close to unity. This strongly argues that the Ce 4f electrons in these compounds are in the nearly localized regime, and may be the origin of the missing 4f intensities in the near-E_F part of the ARPES spectra. In the ARPES spectra, because they are more surface sensitive than 3d-4f RPES, the Ce 4f states should be more localized, and most of the Ce 4f spectral weight would be distributed at deeper binding energies. We also note that although both spectra are very similar, the f^1 to f^0 intensity ratio is somewhat large in $CeIrIn_5$ compared with that of $CeRhIn_5$. This indicates that the hybridization between the conduction electrons and the Ce 4f electrons in $CeIrIn_5$ is slightly stronger than that in $CeRhIn_5$. This suggests that although the Ce 4f states in these compounds are very similar, the hybridization is a little stronger in $CeIrIn_5$ than in $CeRhIn_5$. This is consistent with the fact that $CeIrIn_5$ corresponds to $CeRhIn_5$ under pressure.

Finally, we discuss the relationship between the present results and other experimental results. In the ARPES study of Moore *et al.*[10] on $CeRhIn_5$, the results in the Γ-M direction are essentially identical to our results. They have assigned the quasi-2D FS's to a 4f derived band, and suggested that the results can be understood by itinerant 4f-electron model. However, as discussed in the present paper, the contribution from Ce 4f states for these quasi-2D FS's are very small, and we consider that their results can be understood by the localized 4f-electron model also. Our photoemission experiments suggest that Ce 4*f* electrons are nearly localized not only in $CeRhIn_5$ but also in $CeIrIn_5$. This is consistent with the results of the dHvA experiment on $CeRhIn_5$,[7,6] where the Ce 4*f* electrons are localized, while it is inconsistent with the results on $CeIrIn_5$,[8] where the result was well explained by the itinerant 4*f*-electron model. We consider that this discrepancy may arise from the difference in the measured temperature range. The sample temperature in the dHvA experiment was 25 mK, where the heavy quasi-particle band may be formed. Since the Ce 4*f* electrons in $CeIrIn_5$ are considerably localized, characteristic temperature for the formation of the heavy quasiparticle band should be very low, and probably our photoemission experiments performed at 15K were not able to detect such low-energy phenomena. On the other hand, Zheng *et al.*[9] have measured the temperature dependence of the $1/T_1$ of $CeIrIn_5$, and found the strong temperature dependence (close to $T^{1/2}$) in a temperature range $0.4 \leqslant T \leqslant 100$ K. They have interpreted this behavior as a result of the screening of localized 4*f* moment, and the formation of quasiparticle band in this temperature range. However, our present results suggest that Ce 4*f* electrons in this compound are nearly localized, for example, compared with a low T_K compound such as $CeRu_2Si_2$ ($T_K = 22$ K). Therefore, we suggest that this behavior may arise from another origin, such as spin fluctuations near the AF instability as proposed in Ref. 15.

IV. CONCLUSION

In conclusion, we have found that the Ce 4*f* electrons in these compounds are essentially localized. Although the hybridization between the Ce 4*f* states and conduction electron in $CeIrIn_5$ is somewhat stronger than that in $CeRhIn_5$, it is much weaker than those of a low T_K compound such as $CeRu_2Si_2$.

ACKNOWLEDGMENTS

The authors would like to acknowledge useful discussion with Z.-q. Zheng and J. W. Allen for informative discussion. They also thank A. Sekiyama for allowing to use their spectrum of $CeRu_2Si_2$.

[1] M. D. Mathur, F. M. Groshe, S. R. Julian, I. R. Waker, D. M. Freye, R. K. W. Haselwimmer, and G. G. Lozanrich, Nature (London) **394**, 39 (1998).

[2] S. S. Saxena, P. Agarwal, K. Ahilan, F. M. Grosche, R. K. W. Haselwimmer, M. J. Steiner, E. Pugh, I. R. Walker, S. R. Jolian, P. Monthoux, G. G. Lozanrich, A. Huxley, I. Sheikin, and J. Flouquet, Nature (London) **406**, 587 (2000).

[3] I. R. Walker and F. M. Grosche, Physica C **282–287**, 303 (1997).

[4] H. Hegger, C. Petrovic, E. G. Moshopoulou, M. F. Hundley, J. L. Sarrao, Z. Fisk, J. D. Thompson, Phys. Rev. Lett. **84**, 4986 (2000).

[5] U. Alver, R. G. Goodrich, N. Harrison, D. W. Hall, E. C. Palm, T. P. Murphy, S. W. Tozer, P. G. Pagliuso, N. O. Moreno, J. L. Sarrao, and Z. Fisk, Phys. Rev. B **64**, 180402 (2001).

[6] H. Shishido, R. Settai, D. Aoki, S. Ikeda, H. Nakawaki, N. Nakamura, T. Iizuka, Y. Inada, K. Sugiyama, T. Takeuchi, K. Kindo, T. C. Kobayashi, Y. Haga, H. Harima, Y. Aoki, T. Namiki, H. Sato, and Y. Ōnuki, J. Phys. Soc. Jpn. **71**, 162 (2002).

[7] C. Petrovic, R. Movshovich, M. Jaime, P. G. Pagliuso, M. F. Hundley, J. L. Sarrao, Z. Fisk, and J. D. Thompson, Europhys. Lett. **53**, 354 (2001).

[8] Y. Haga, Y. Inada, H. Harima, K. Oikawa, M. Murakawa, H. Nakawaki, Y. Tokiwa, D. Aoki, H. Shishido, S. Ikeda, N. Watanabe, and Y. Ōnuki, Phys. Rev. B **63**, 060503 (2001).

[9] G. -q. Zheng, K. Tanabe, T. Mito, S. Kawasaki, Y. Kitaoka, D. Aoki, Y. Haga, and Y. Onuki, Phys. Rev. Lett. **86**, 4664 (2001).

[10] D. P. Moore, T. Durakiewicz, J. J. Joyce, A. J. Arko, L. A. Morales J. L. Sarrao, P. G. Pagliuso, J. M. Wills, and C. G. Olson, Physica B **312–313**, 134 (2002).

[11] D. Hall, E. C. Palm, T. P. Murphy, S. W. Tozer, C. Petrovic, E. M-Ricci, L. Peabody, C. Q. H. Li, U. Alver, R. G. Goodrich, J. L. Sarrao, P. G. Pagliuso, J. M. Wills, and Z. Fisk, Phys. Rev. B **64**, 064506 (2001).

[12] O. Gunnarsson and K. Schönhammer, Phys. Rev. B **28**, 4315 (1983).

[13] A. Sekiyama, T. Iwasaki, K. Matsuda, Y. Saitoh, Y. Ōnuki, and S. Suga, Nature (London) **403**, 396 (2000).

[14] J. J. Yeh and I. Lindau, At. Data Nucl. Data Tables **32** (1985).

[15] Y. Kohori, Y. Yamato, Y. Iwamoto, T. Kohara, E. D. Bauer, M. B. Maple, and J. L. Sarrao, Phys. Rev. B **64**, 134526 (2001).